European Polymer Journal 205 (2024) 112758

Contents lists available at ScienceDirect

European Polymer Journal

journal homepage: www.elsevier.com/locate/europolj

Oligo(ethylene glycol) methyl ether methacrylate based hydrogel with intrinsic antibacterial activity against *Pseudomonas aeruginosa* as a model of a major wound infecting human pathogen

Ahmet Çetinkaya [a], Ann-Kathrin Kissmann [b], Magdalena Lipinska [a], Marta Trzaskowska [c], Jan Duniec [a], Hitesh Katariya [a], Miroslav Slouf [d], Tilmann Herberger [e], Tanja Weil [e], Agata Przekora [c], Frank Rosenau [b,*], Joanna Pietrasik [a,*]

[a] Institute of Polymer and Dye Technology, Lodz University of Technology, Stefanowskiego 16, 90-537 Lodz, Poland
[b] Institute of Pharmaceutical Biotechnology, Ulm University, Meyerhofstrasse 1, 89081 Ulm, Germany
[c] Independent Unit of Tissue Engineering and Regenerative Medicine, Medical University of Lublin, Chodzki 1, 20-093 Lublin, Poland
[d] Institute of Macromolecular Chemistry, Czech Academy of Sciences, Heyrovskeho namesti 2, 162 06, Praha 6, Czech Republic
[e] Max Planck Institute for Polymer Research, Ackermannweg 10, Mainz 55128, Germany

ARTICLE INFO

Keywords:
Biocidal surfaces
Wound healing
Quaternization
Wound dressing
Gels
P. aeruginosa

ABSTRACT

Wound dressings represent the first important defense line against potentially life-threatening infections. Successful materials should unify efficiency, simplicity of production with the ease of application. Cationic polymers based on quaternary ammonium salt moieties along the polymer chain promise high efficacy against growth of relevant pathogens including drug-resistant strains. We present a novel and easy-to-handle wound dressing material based on the well-defined copolymers of oligo(ethylene glycol) methyl ether methacrylate (OEGMA) and 2-(dimethylamino)ethyl methacrylate (DMAEMA), using quaternization with 1,6-dibromohexane for hydrogel formation. The material obtained from this robust approach was perfectly biocompatible with human dermal fibroblasts and revealed an auspicious degree of intrinsic antibacterial activity against *P. aeruginosa* as a model pathogen for hospital-acquired infections. Formation of bacterial biofilms was prevented in early- and late-stages and even planktonic cells were killed upon gel contact. The rheological properties of the hydrogel materials were comprehensively characterized in both dry and swollen states. Excellent biological performance and appropriate viscoelastic properties qualify the hydrogels from our production approach as truly promising novel wound dressing materials with long-lasting and contact-active bactericidal activities. We believe that this charmingly simple procedure and the mechanical properties of the hydrogel may open new avenues towards cost-effective next-generation first-line wound-care materials.

1. Introduction

Microbial infections have emerged as one of the main health threats of our time, with nosocomial infections representing the most challenging tasks to be managed by healthcare facilities, especially intensive care units that handle truly severe injuries, including large burn wounds [1,2]. In particular, according to the World Health Organization (WHO), infections are the second leading cause of mortality worldwide, and according to the European Centre for Disease Control (ECDC), more than 4 million patients are affected by nosocomial infections every year in Europe alone [3], with immune suppressed patients being the most threatened individuals.

Although wounds become chronic due to various reasons, they share some common parameters. Hard-healing wounds are characterized by high levels of pro-inflammatory cytokines, reactive oxygen species (ROS), and matrix metalloproteinases (MMPs). Prolonged healing is also the result of insufficient tissue vascularity, infection, and tissue necrosis [4–8]. Colonization of the wound by bacteria is a particularly dangerous factor that hinders tissue regeneration not only because pathogenic bacteria can stimulate the inflammatory process but also because they are an attractant for leukocytes synthesizing cytokines, ROS, and proteases that lead to the destruction of the infected tissue [9]. A major

* Corresponding authors.
E-mail addresses: frank.rosenau@uni-ulm.de (F. Rosenau), joanna.pietrasik@p.lodz.pl (J. Pietrasik).

https://doi.org/10.1016/j.eurpolymj.2024.112758
Received 1 November 2023; Received in revised form 3 January 2024; Accepted 8 January 2024
Available online 11 January 2024

pathogen that is normally acquired in hospital environments with enormous pathogenic potential is the gramme-negative bacterium *P. aeruginosa*, which, due to its ability to produce an impressive arsenal of toxins and other secreted virulence factors, was among the first bacteria whose large genome was sequenced in the early 2000s [10]. *P. aeruginosa* PAO1 like many other *Pseudomonas* pose a considerable additional threat to patient welfare, which originates from its intrinsic lifestyle preference to form elaborated multicellular biofilms on surfaces (e.g. wound surfaces, medical equipment) that allow it to persist under harsh conditions [11,12]. *P. aeruginosa*, especially due to mutations against last resort antibiotics such as carbapenem, has been identified as a major global health threat and is therefore on the WHO priority list of the most threatening pathogens with the highest demand for novel antibiotics and treatment [13].

Despite the shockingly high number of cases and the severity of individual health consequences, mankind requires novel procedures, methods, and materials to meet this tremendous health problem. Undoubtedly, the best infection treatment is to avoid the development of full infections, which means to exclude or significantly inhibit early infection stages. In clinical wound care, a significant focus has been put on novel surgical (wound) dressings as first defense lines against major (nosocomial) problematic human pathogens [14–17].

The selection of the appropriate dressing according to the characteristics of the wound is an important element of the treatment process [18]. Many materials have been used for rapid wound healing, including porous foams, biocompatible membranes, electrospun nanofibers, and functional hydrogels [19–25]. Hydrogels have come to the forefront among these biomaterials due to their properties such as absorbing tissue exudates, keeping the wound environment moist, cooling the surface, having decent mechanical parameters, allowing oxygen to penetrate [26–30].

Recently, we have introduced antimicrobial hydrogel composite materials functionalized with affinity molecules facing the wound and consequently, the pathogen freshly starting its development toward a full and potentially deadly infection. These so-called 'capture-and-kill' concepts are based on (specific) binding of bacterial or yeast cells with lectins or aptamers [15,16,31]. The aim is to remove the early stages of infection together with the wound dressing during the standard daily exchange procedure. This removal of immobilized cells is conceptually safeguarded by a second defense line which is realized by loading the gels with appropriate antimicrobial drugs (e.g., antibiotics or antimicrobial peptides). These drug-loaded composite constructs have intrinsic drawbacks residing in their complexity and resulting from that in material costs of the final product which may render them economically unattractive. In this context, hydrogels with inherent antimicrobial activity, for example positively charged polymers, constitute valuable alternatives for real applications on the mid-term time scale [32–34]. In addition to these properties, it should be painless and hassle-free to change the gels used as wound dressings during the application, therefore it is important to prepare the gels as a thin film [35–40].

Contact-active biocidal materials kill bacteria through direct contact with the bacterial membrane and have received great attention due to their environmental friendliness and their long-term durability [41–44]. Among the various biocidal materials developed so far, cationic polymers carrying quaternary ammonium salt moieties along the polymer chain have been shown to exhibit high efficacy in inhibiting the growth of drug-resistant microbes [45–50]. Due to their multifunctionality, biocompatibility, and immunogenic nature, they have attracted great interest in the prevention and/or treatment of bacterial diseases [51]. Quaternized poly(2-(dimethylamino) ethyl methacrylate) (PDMAEMA) and its derivatives have been extensively studied as effective antimicrobial materials [52–55]. Such polymers provide an ideal platform for the development of long-lasting, contact-active bactericidal surfaces [56].

In this study we developed very robust and simple wound dressing system based on well-defined copolymer of oligo(ethylene glycol) methyl ether methacrylate (OEGMA) and 2-(dimethylamino)ethyl methacrylate (DMAEMA) utilizing quaternization with 1,6-dibromohexane for hydrogel formation. Notably, the obtained hydrogel significantly addressed the need for hydrophilic, immunogenic, and non-cytotoxic polymers with intrinsic antibacterial activities against *P. aeruginosa*. Moreover, the proposed approach allows to obtain the discussed material under mild conditions. Since the P(OEGMA-*stat*-DMAEMA) copolymer was synthesized via reversible addition-fragmentation chain-transfer polymerization (RAFT) the gel demonstrated a very uniform structure. The viscoelastic properties of the synthesized gels with varied amounts of crosslinkers, 1,6-dibromohexane, were investigated and discussed. In addition, the results of biological tests verified the designed biomaterial as a promising new material for wound dressing applications. Inhibition tests against *P. aeruginosa* bacteria, biocompatibility on healthy cells, and proliferation mechanisms upon healthy cell culture reported within this work.

2. Materials and methods

2.1. Materials

Monomers: oligo(ethylene glycol) methyl ether methacrylate ($OEGMA_{300,}$ 98%) and 2-(dimethyl amino)ethyl methacrylate (DMAEMA, 98%) were purchased from Sigma Aldrich and filtered on basic alumina to remove butylated hydroxytoluene (BHT) and 4-methoxyphenol (MEHQ) inhibitors prior the usage. 2-Cyano-2-propyl benzodithioate (CPBD, 99%), 2,2′-azobis(2-methylpropionitrile) (AIBN, 98%), and 1,6-dibromohexane (98%) were purchased from Sigma Aldrich and used as received. The N,N-dimethylformamide (DMF, 99.8%) and n-hexane (99%) solvents were provided by Avantor Performance Materials Poland. Dry tetrahydrofuran (THF, 99.8%) was purchased from Sigma Aldrich and used as received.

2.2. Methods

2.2.1. Preparation of the thin film gels

The copolymers of poly(oligo(ethylene glycol) methyl ether methacrylate)-*stat*-poly(2-(dimethylamino)ethyl methacrylate), (POEGMA-*stat*-PDMAEMA), were synthesized by RAFT polymerization of OEGMA and DMAEMA monomers. Briefly, the gels were obtained by quaternization of the obtained copolymers with 1,6-dibromohexane in THF. Fig. 1**A** and Fig. 1**B** represent the gel synthesis procedure. Detailed methods are given in the supporting information.

2.2.2. Characterizations

^{1}H nuclear magnetic resonance (^{1}H NMR), gel permeation chromatography (GPC), a light microscopy (LM) and cryogenic scanning electron microscopy (cryo-SEM), dynamic rheological measurements and swelling ratio tests were conducted to characterize the copolymer samples or gels. The detailed methods are described in the supporting information.

2.2.3. Biocompatibility tests

The details of cell culture procedure of human skin fibroblasts (BJ cell line, ATCC), cytotoxicity evaluation and assessment of cell proliferation tests are given in supporting information.

2.2.4. Anti-Pseudomonas properties

Cultivation of *P. aeruginosa* PAO1 pVLT31-eGFP [57] bacterium, *P. aeruginosa* PAO1 attachment and biofilm maturation inhibition assay, Planktonic *P. aeruginosa* PAO1 viability reduction test, and *P. aeruginosa* POA1 contact toxicity – collagen matrix model tests are presented in the supporting information with details.

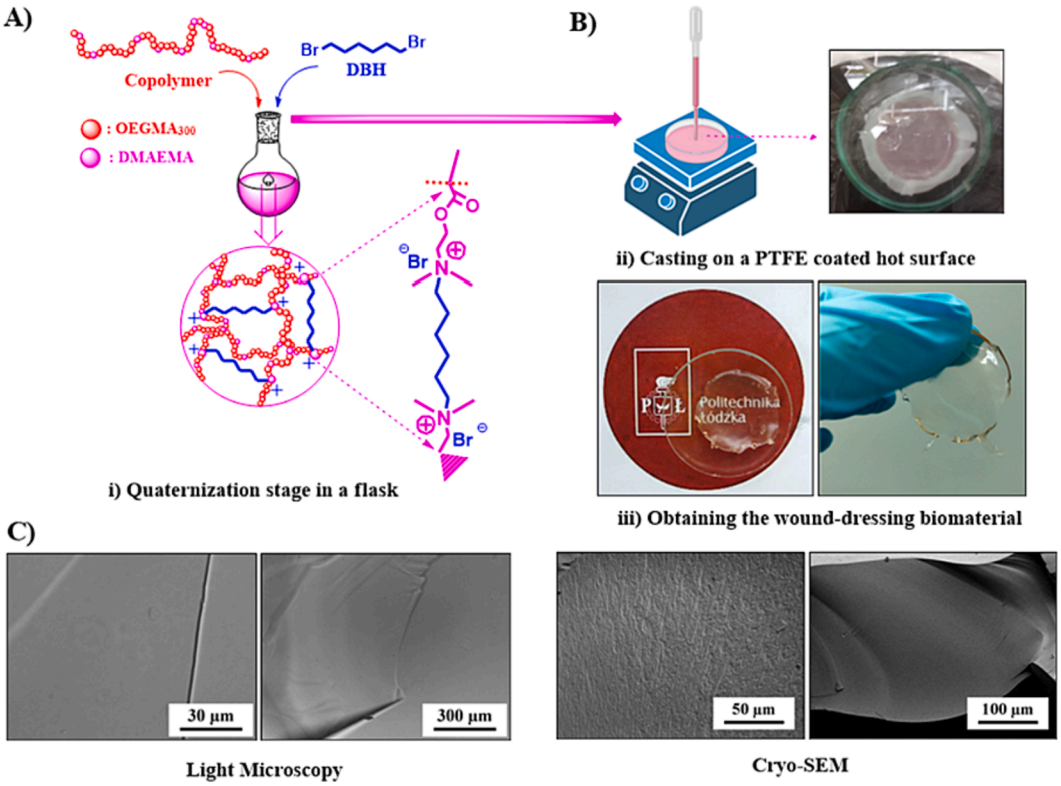

Fig. 1. The scheme for the synthesis of gel films based on P(OEGMA-*co*-DMAEMA) and their microscopical analysis. A) Quaternization was initially carried out in an inert flask. B) As soon as the solution became viscous it was transferred to a Teflon-coated hot glass surface to form a film. C) Light-microscopy and cryo-SEM images of obtained gels.

3. Results and discussion

3.1. Molecular characterization of the gels

Wound dressings with antibacterial and multifunctional abilities that can accelerate the healing process are urgently needed. Herein the very robust and simple wound dressing system based on the polymer gel was designed to demonstrate the intrinsic antibacterial activities against *P. aeruginosa.* To control and reduce the heterogeneity of the formed polymer network, it was generated as a result of the post-polymerization crosslinking of well-defined linear copolymers. To obtain water-swellable gels, poly(oligo(ethylene glycol)methyl ether methacrylate-*stat*-poly(2-(dimethylamino)ethyl methacrylate), (POEGMA-*stat*-PDMAEMA) copolymer was synthesized and then used for the gel formation. Reversible addition-fragmentation chain transfer (RAFT) polymerization was used to form well-defined linear chains (Fig. S1). The copolymer composition was designed in such a way that DMAEMA units were applied to form crosslinks within the gel by quaternization, while OEGMA units were responsible for water adsorption. The applied monomer ratio in the polymerization mixture was set up to OEGMA/DMAEMA = 5/1 mol/mol. The molecular weight of the copolymers obtained was in the range of M_n = 60,000 g/mol, with a molecular weight distribution $Đ < 1.30$. The GPC plots were symmetric, showing good control over the polymerization as shown for the arbitrarily chosen sample (Fig. S2). The content of DMAEMA units in the final copolymer was calculated based on its ^{1}H NMR spectrum (Fig. S3). For this purpose, the ratio of the integral of the terminal methyl groups (–O–CH_3) (3.42–3.32 ppm) (δ = 3.36 ppm) belonging to the OEGMA units to the protons of the terminal methyl groups (–N–$(CH_3)_2$) (δ = 2.22 ppm) was compared. Consequently, DMAEMA content within the copolymer was determined to be 20 mol%. Next, using 1,6-dibromohexane in the crosslinking step (Fig. S4), thin films were prepared using a very simple and feasible setup. Fig. 1**A** and Fig. 1**B** present the chemical structure of the formed gels, as well as the setup for the film generation and gel appearance. Two independent microscopic techniques (light microscopy of samples submerged in water and cryogenic scanning electron microscopy of samples vitrified in slush nitrogen) demonstrated that the morphology of all investigated gels was uniform and homogeneous (Fig. 1**C**). The crosslinking density of the synthesized gels was varied through the amount of the crosslinker used, 1,6-dibromohexane, for the gel formation and was reflected by the swelling ratio values. It appeared the high access of crosslinker, 16 eq., versus DMAEMA units, did not influence the swelling ratio because it was the same or even slightly smaller in comparison to the system containing 12 eq. or 2.2 eq. of 1,6-dibromohexane (Table 1). However, only such gels, crosslinked by using 16 eq., were macroscopically stable in the buffer solutions after long storage; more than 48 h. It was assumed that the observed effect could be due to the variation within the gel morphologies produced when different concentrations of crosslinker were used.

The performance of the synthesized gels was investigated based on the viscoelastic properties in dry and wet states, respectively, because when hydrogels absorb wound exudate, swelling of the gel occurs and affects the surrounding tissue, therefore the healing process. This type of test was also used for the optimization of the amounts of the used crosslinkers. The only gel that was stable in buffer after a long storage time (gel 3) was subjected to rheological tests in the swollen state.

3.2. Viscoelastic properties of the gels

3.2.1. The effect of the crosslinker amount in dry state

Based on the amplitude sweep test at a constant angular frequency of 10 rad/s at ambient temperature the values of the storage shear modulus G' (kPa), the loss shear modulus G'' (kPa) and tan δ (-), complex viscosity η* (Pas), dynamic viscosity η' (Pas) for the linear viscoelastic region were determined. The calculated average values of viscoelastic parameters for studied gels are compiled in Table 1. The viscoelastic parameter

Table 1
The viscoelastic characteristic of the synthesized gels.

Gel	Crosslinker	Swelling ratio	G'_{LVR} (kPa)	G''_{LVR} (kPa)	Tan δ (-)	Complex viscosity η^*_{LVR} (Pas)	Dynamic viscosity η'_{LVR} (Pas)
1 (NS[a])	2.2 eq.	8.8x	17.47 ± 0.32	4.56 ± 0.10	0.261 ± 0.005	1805.4 ± 31.8	456.0 ± 9.5
2 (NS[a])	12 eq.	6.5x	12.77 ± 0.44	5.64 ± 0.19	0.441 ± 0.002	1395.8 ± 48.2	563.5 ± 18.9
3 (S[b])	16 eq.	6.5x	19.73 ± 0.23	10.34 ± 0.06	0.524 ± 0.004	2227.8 ± 23.0	1033.7 ± 6.4
3 swollen	16 eq.	6.5x	19.52 ± 0.20	0.39 ± 0.05	0.020 ± 0.002	1953.0 ± 19.8	39.2 ± 4.9

[a] NS- not stable in buffer solution after 48 h.
[b] S-stable in buffer solution after 48 h.

values determined for the oscillation strain range of up to 5% were used to calculate the average values.

All studied samples showed the linear behaviour for the studied oscillation frequency range, no significant changes of G' and G'' values were detected up to 10% of deformation. The highest average value of the storage shear modulus G' for gel 3 crosslinked by 16 eq. of 1,6-dibromohexane indicated the highest crosslinking density of the gel compared to those crosslinked by a lower amount of 1,6-dibromohexane. Furthermore, a stronger dissipation of the energy was observed, reflected by an average value of the loss shear modulus G'' that was twice as high. That was probably due to different topology of the formed gel network and changes in chain mobility. The damping properties of the material were better as it is reflected by higher values of tan δ (Table 1, Fig. S5). As it was observed, the tan δ values determined for gel 1 crosslinked by the lowest amount, 2.2 eq. of 1,6-dibromohexane were oscillating at low oscillation strain, less than 2% of the oscillation strain. This indicates that changes in the structure of the material occurred, probably because of the damage of the formed network. The gel 3 showed better dynamic mechanical stability, no significant changes in the values of tan δ were observed (Fig. S5**C**).

The application of higher amounts of crosslinkers, 16 eq., led to a significant increase of dynamic viscosity η', which is twice as high as gels crosslinked by 2.2 eq. and 12 eq. of 1,6-dibromohexane (Fig. S6). To further analyse the influence of the amount of the crosslinkers on the viscoelastic properties the frequency sweep tests were performed at ambient temperature (Fig. 2). For all gels studied, the values of the storage shear modulus G' were higher than the values of the loss modulus G'' in the whole studied frequency range, identifying the predominant elastic behaviour. The values of storage shear modulus G' and loss shear modulus G'' decreased as the applied angular frequency was lower (the long relaxation time) indicating smooth and undisturbed relaxation of the material. In the high-frequency range, where the elastic behaviour of the material is more predominant, gel 3 showed the highest values of the storage shear modulus due to the higher amount of crosslinks in the gel network. Furthermore, for gel 3 crosslinked by 16 eq. of 1,6-dibromohexane, the values of the loss shear modulus G'' were significantly higher compared to gels crosslinked using a lower amount of 1,6-dibromohexane.

The plots of complex viscosity η* (Pas), dynamic viscosity η' (Pas) and loss factor tan δ (-) as a function of angular frequency are included in the supporting information (Fig. S7). All the gels studied showed a shear thinning behaviour, the values of dynamic viscosity and complex viscosity decreased as the higher values of frequency (higher shear rate) were applied (Fig. S7). The higher amount of crosslinker used, 16 eq. (gel 3), strongly influenced the dynamic viscosity η' of crosslinked gel measured as a function of the angular frequency (Fig. S7). For the gel samples crosslinked by 2.2 eq. and 12 eq. the lower values of dynamic viscosity η' were observed at higher values of frequency. It suggests a lower concentration of crosslinks present in the network structure of both gels. The effect on the complex viscosity η* was less visible, here the increase of the complex viscosity η* values was observed for the applied frequency range higher than 50 rad/s. The higher angular frequency at a similar level of oscillation strain generates a higher shear rate, as the viscosity for most of the polymeric material decreases as the shear rate is higher (shear thinning behaviour). The higher level of viscosity at a similar level of frequency indicates the higher crosslinking density of the material.

3.2.2. *The viscoelastic properties of the gel at a swollen state*

The only gel that was stable in buffer after a long storage time (gel 3) was subjected to rheological tests in the swollen state (Fig. S8). The presence of the solvent strongly influenced the dissipation of the energy by the swollen material. Here, it was observed that the presence of buffer did not strongly affect the values of the storage shear modulus G', but the decrease in the values of the G' parameter started at a lower value of the oscillation strain compared to dry gel 3 (Fig. S9). The calculated average values of G' for the linear viscoelastic region were very similar (Table 1) and the presence of buffer had no meaningful influence on the elasticity of the material in the linear viscoelastic region. Oppositely, the presence of buffer drastically decreased the values of the loss modulus G'' at low values of the oscillation strain (linear viscoelastic region). The higher applied oscillation strain led to an increase in the loss shear modulus

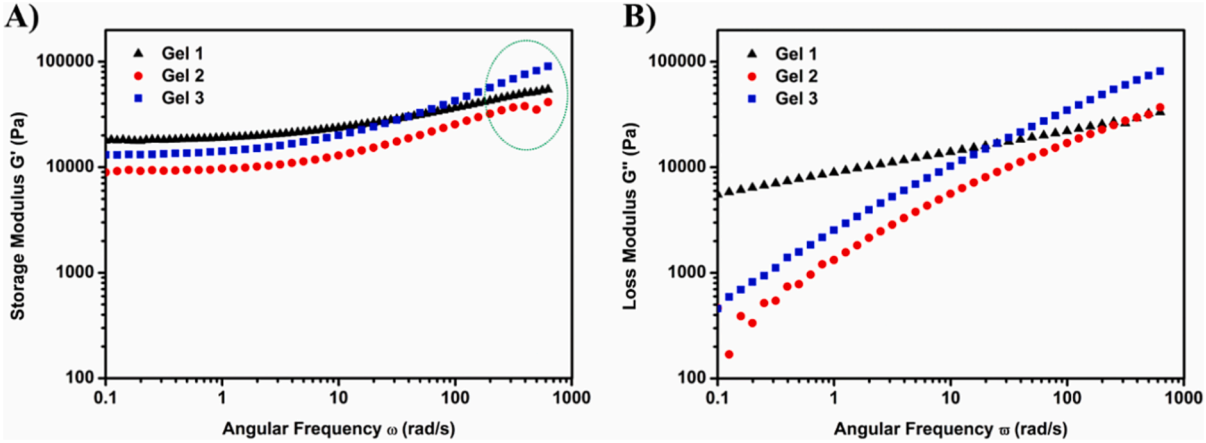

Fig. 2. The values of the storage shear modulus G' (Pa) and the loss shear modulus G'' (Pa) as a function of applied angular frequency (rad/s). Applied constant oscillation strain 0.1%; samples gel 1 (2.2 eq), gel 2 (12 eq) and gel 3 (16 eq).

probably because of the removal of the buffer from the structure of the swollen gel.

The presence of buffer affected the dynamic viscosity of the material, the calculated value of $\eta^{'}$ for the low oscillation strain (low shear rate) was 39.2 Pas and increased up to the value of 615 Pas for the 5% of oscillation strain, probably due to the removal of the solvent from the structure of the gel. The complex viscosity η* (Pas) measured as a function of angular frequency decreased when high frequency values were applied during the test. A similar trend was observed in the case of the dynamic viscosity $\eta^{'}$ (Pas). The changes in the viscosity of the gel after swelling were due to the presence of the buffer being trapped in the structure of the crosslinked gel (**Fig. S10**). It can be noticed that the presence of the buffer in the structure of the gel affected the G* values only in the high-frequency range (**Fig. S11A**). At low frequency due to the longer time, the relaxation of the swollen material was not disturbed and the differences in the $G^{'}$ values of the dried as well as the swollen gel were less significant. A stronger elastic dynamic response of the dried gel was observed for higher angular frequency values (higher than 10 rad/s) and the increase of the $G^{'}$ modulus compared to the swollen gel was detected. In contrast, the swelling of the gel strongly influenced the values of the loss modulus. The viscous behaviour of the material changed drastically due to the buffer molecules that were trapped within the structure. The lower values of the loss shear modulus $G^{''}$ were determined for the entire studied frequency range compared to the dry material. It was clear that the presence of the buffer affected the dissipation of the energy during the deformation of the swollen gel.

3.3. Biocompatibility tests

Cell culture experiments clearly proved that gel 3 was not cytotoxic to skin fibroblasts since cell viability was approximately 90% after 24 h of exposure and exceeded 100% after 48 h of incubation in the presence of the material extract (Fig. 3**A**). Higher cell viability compared to control cells after 48 h exposure time was most likely the result of an increase in the number of cells in the population in response to gel 3. This assumption was proven in the proliferation assay, where a greater number of extract-treated cells was observed after 48 h of incubation compared to control cells (Fig. 3**B**). Importantly, it was demonstrated that the cells cultured in the presence of the material extract showed a significantly higher proliferation rate, which was reflected by the calculated proliferation parameters (doubling time – DT and growth rate – GR), (Table 2). DT estimated for extract-treated cells was significantly shortened to approx. 36 h compared to the control fibroblasts (approx. 44 h). Biocompatibility of the biomaterial was also confirmed in direct contact tests by live/dead fluorescent staining. The experiment revealed that gel 3 was not only unsupportive to cell adhesion, which is a desired phenomenon in the case of wound dressings but also noncytotoxic to skin fibroblasts. The lack of cell adhesion was confirmed by the presence of a small number of spherical cells on the surface of gel 3 (Fig. 3**C**). Importantly, the cells showed green fluorescence, proving the non-cytotoxicity of the material. On the contrary, cells cultured on the polystyrene well next to gel 3 showed high viability (green fluorescence) and typical morphology of healthy, well-attached fibroblasts (Fig. 3**D**), which was similar to the morphology of the control cells (Fig. 3**E**). It is another evidence that the tested material was not cytotoxic.

The performed biocompatibility tests clearly proved the high biomedical potential of gel 3. The material was not cytotoxic to the cells, it enhanced cell proliferation and finally did not allow for fibroblast

Table 2
Comparison of proliferation rate between control cells and fibroblasts exposed to the extract of gel 3.

Parameter	Control	Gel 3
Doubling Time (hours)	44.11	35.63
Growth Rate	0.0157	0.0195

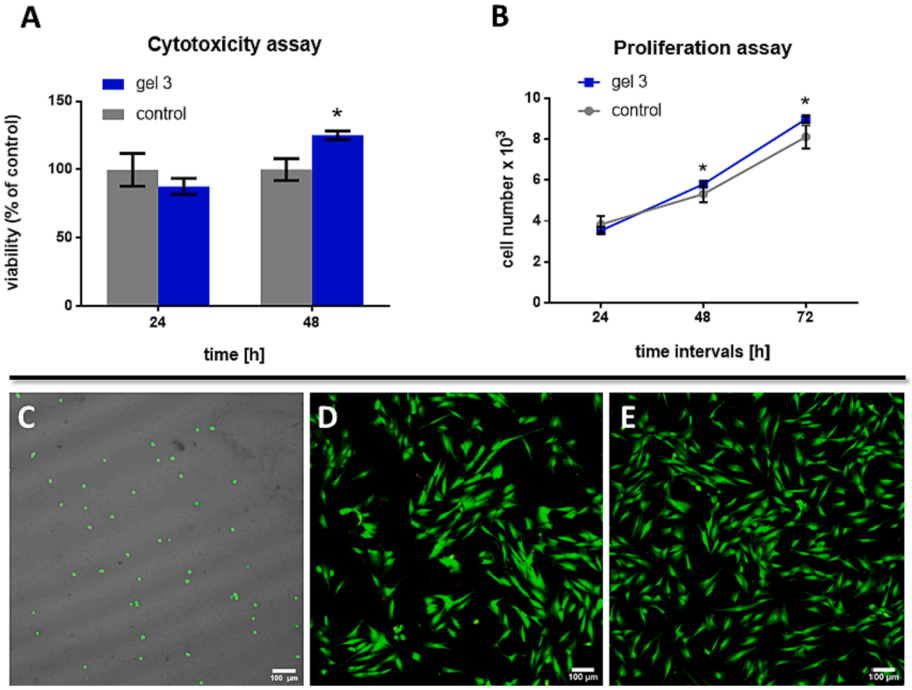

Fig. 3. Assessment of biocompatibility of the material: (A) cytotoxicity test results of the gel 3 extract against human skin fibroblasts (BJ cell line) evaluated by WST-8 assay, *statistically significant results compared to control by unpaired *t*-test, $p < 0.05$. (B) evaluation of cell proliferation after exposure to gel 3 extract by LDH total assay, *statistically significant results compared to control by unpaired *t*-test, $p < 0.05$. (C) confocal microscopy images of BJ cells cultured on the surface of gel 3, (D) on the polystyrene well next to the gel 3, and (E) on the polystyrene well (control cells) after live/dead double staining, magn. 100×. Viable cells show green fluorescence, dead cell nuclei show red fluorescence. (For interpretation of the references to colour in this figure legend, the reader is referred to the web version of this article.)

attachment to its surface. All mentioned features are of high importance considering the dressing material's clinical applications. Increased fibroblast proliferation is desired as it ensures the regeneration of difficult-to-heal wounds [58]. In turn, hindered fibroblast adhesion to the surface of wound dressings is crucial since it ensures painless dressing removal after completed healing [18].

3.4. Anti-Pseudomonas properties

P. aeruginosa is known to form biofilms with elaborate architectures during the maturation process. Biofilm formation, however, starts with the attachment of planktonic cells after they have been released from older biofilms or, e.g., when cells have been introduced externally from the environment, as is the case during the onset of infections on wounds (Fig. 4**A**). The synthesized novel gel material, gel 3, was tested with both relevant stages, early attachment of GFP expressing fluorescence labelled *P. aeruginosa* cells and older biofilms (24 h) of the same recombinant strain in comparison to surfaces of traditional commercial cell culture material (i.e., polystyrene). Whereas in both situations fluorescent *P. aeruginosa* was detected on the plastic material, the surface of investigated gel 3 was completely free from bacteria and no signal was visible (Fig. 4**B**) indicating that the gel had inhibited both the attachment of cells in the early biofilm stage and the maturation of typical multicellular biofilms. In a submersion assay, the material samples were submerged into a starting culture of dispersed *P. aeruginosa* cells at low cell densities (optical density at 600 nm) and allowed to grow above the gel and the plastic control. The final cell densities were determined and, in parallel, a live-dead assay was applied to measure the proportion of viable cells in these cultures. To exclude the harmful effects of compounds from the gel preparation (DMF) the gels were directly used or washed and equilibrated in the aqueous phase prior to use (Fig. 4**C**). A control equilibration experiment had, as expected, no significant effects on cells grown over the polystyrene material of the standard culture cultivation plates. The same was observed for gel 3 confronted cultures, which reached the same cell densities with or without equilibration. However, compared to the grown on polystyrene material controls, the gel 3 culture was obviously strongly reduced in growth with drastically reduced final cell densities (Fig. 4**C, left graph**). Furthermore, compared to the polystyrene control culture, cells almost completely lost their viability, when grown over gel material independent of equilibration (Fig. 4**C, right graph**), indicating that the presence of the material has inhibitory effects on *P. aeruginosa* cells in the planktonic phase (i.e., in the liquid phase) even when it is not the direct substratum of a developing biofilm. Antibacterial properties of the biomaterial were also proven using collagen matrix model. The test revealed that there were no viable bacteria on all investigated surfaces: 1) biomaterial surface that was in contact with *P. aeruginosa*-inoculated collagen matrix, 2) surface of *P. aeruginosa*-inoculated collagen matrix that was in the contact with tested hydrogel, and 3) surface of the *P. aeruginosa*-inoculated collagen matrix that was not in contact with the biomaterial but was located next to the tested hydrogel (Fig. 4**D**).

The cell wall of gram-negative bacteria contains lipopolysaccharide moieties with lipid A as the core element of the molecule [59]. Phosphate groups coordinate Mg^{2+}-counter-ions and thus stabilize the outer membrane, delivering a molecular reason for the notorious susceptibility of *P. aeruginosa* towards chelating agents like EDTA which was shown to weaken the structural integrity of *P. aeruginosa* cells [60]). The positively charged groups of gel 3 may serve as attachment sites of the material to lipid A in the membrane of *P. aeruginosa* target cells, thus severely altering the integrity of the membrane and reducing the viability of the bacterial cell.

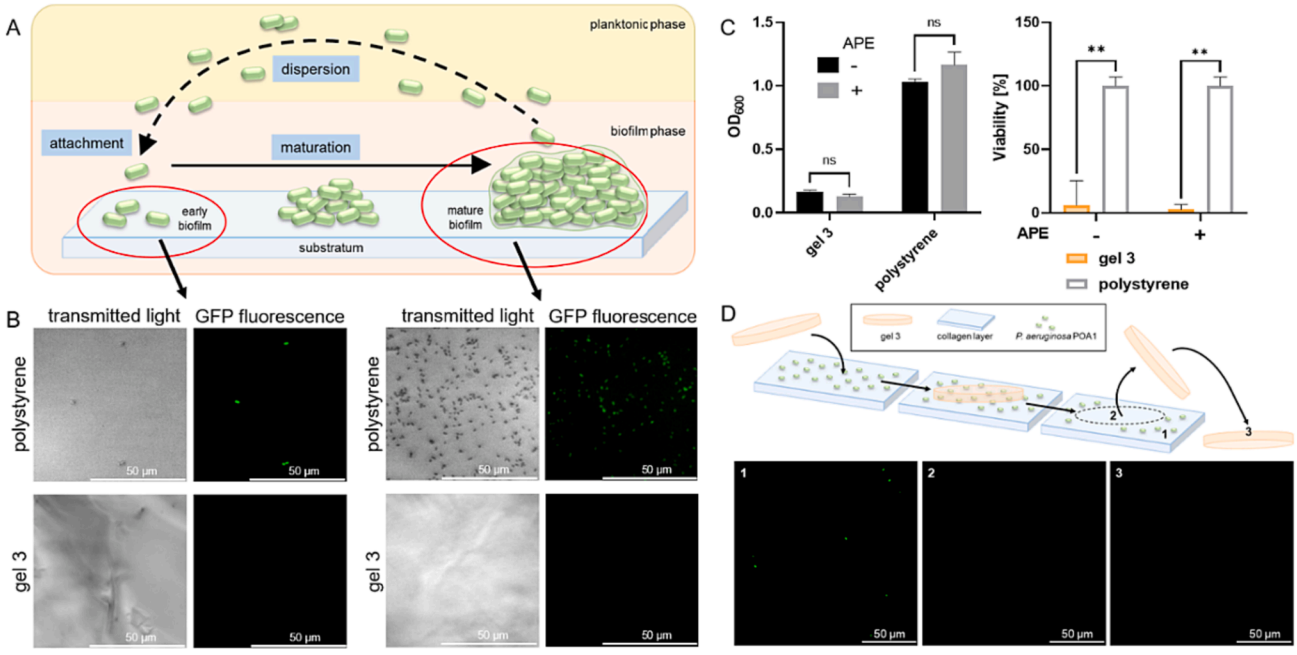

Fig. 4. Anti-microbial properties against *P. aeruginosa*. A) Schematic overview of typical *P. aeruginosa* biofilm formation. First, planktonic cells attach to the surface, then the cells aggregate and start to proliferate until they form a mature biofilm with an extracellular matrix. In order to produce further biofilms, cells can detach (dispersion) from the mature biofilm to serve as seeds for the next generation of future biofilms. B) Microscopic analysis under transmitted light and GFP fluorescence of *P. aeruginosa* PAO1 pVLT31-eGFP after 30 min (attachment phase) or 24 h (mature biofilm phase) of incubation at 37 °C on gel 3 or on standard commercial polystyrene-based cell culture plastic. C) Optical density at 600 nm and viability of *P. aeruginosa* PAO1 after 24 h of incubation with the polymer gels after "aqueous phase equilibration" ("APE") (+) or after ethanol washing (-). Error bars symbolize standard deviations of measurements conducted in triplicates. *P* values of 0.05 were considered as significant. ** denotes 0.01 and n.s. not significant. D) Schematic concept of a collagen-based hydrogel serving as an extracellular matrix model for the binding of pathogenic cells. The matrices were "infected" with *P. aeruginosa* and the polymer gel was applied directly onto the *P. aeruginosa* cells. Position 1: Far remote from the application site. Position 2: Directly under the application site and Position 3: Surface of polymer material after contact. Fluorescence microscopy and bright-field microscopy using the Leica DMi8 inverted fluorescent microscope for each position at 630× magnification.

4. Conclusions

In this study, copolymers of oligo(ethylene glycol) methyl ether methacrylate (OEGMA) and 2-(dimethylamino)ethyl methacrylate (DMAEMA) were utilized for the synthesis of polymer gels. The quaternization reaction was used as an easy and effective method for copolymer crosslinking via 1,6-dibromohexane. The obtained novel biomaterial containing quaternized groups demonstrated high biological potential, improved viscoelastic properties, high stability in aqueous media and inhibitory effects on *P. aeruginosa* cells in the planktonic phase. Therefore, it was concluded that such material is good candidate to be used as a wound dressing in chronic wounds in the management of moderate exudate, providing appropriate moisture and oxygenation, and accelerating the healing process. In addition, it is a decent toolbox for our future studies in terms of the inhibition of drug-resistant bacteria and the development of dressing materials with intrinsic antibacterial properties.

CRediT authorship contribution statement

Ahmet Çetinkaya: Formal analysis, Investigation, Methodology, Writing – original draft. **Ann-Kathrin Kissmann:** Formal analysis, Investigation, Methodology, Writing – original draft. **Magdalena Lipinska:** Formal analysis, Investigation, Methodology, Writing – original draft. **Marta Trzaskowska:** Formal analysis, Investigation, Methodology, Writing – original draft. **Jan Duniec:** Investigation. **Hitesh Katariya:** Investigation. **Miroslav Slouf:** Investigation. **Tilmann Herberger:** Investigation. **Tanja Weil:** Conceptualization. **Agata Przekora:** Conceptualization, Methodology, Supervision, Writing – review & editing. **Frank Rosenau:** Conceptualization, Methodology, Supervision, Writing – review & editing. **Joanna Pietrasik:** Conceptualization, Methodology, Supervision, Writing – review & editing.

Declaration of Competing Interest

The authors declare that they have no known competing financial interests or personal relationships that could have appeared to influence the work reported in this paper.

Data availability

The raw/processed data required to reproduce these findings cannot be shared at this time as the data also forms part of an ongoing study.

Acknowledgment

The financial support from National Science Centre, Poland is gratefully acknowledged (Grant UMO-2020/39/I/ST5/02108). For the purpose of Open Access, the authors have applied a CC-BY public copyright license to any Author Accepted Manuscript (AAM) version arising from this submission. This work was also supported by grant from the German Research Society (DFG) project 465229237.

Appendix A. Supplementary data

Supplementary data to this article can be found online at https://doi.org/10.1016/j.eurpolymj.2024.112758.

References

[1] J.A. D'Abbondanza, S. Shahrokhi, Burn infection and burn sepsis, Surg. Infect. (Larchmt.) 22 (1) (2021) 58–64.
[2] M.P. Rowan, L.C. Cancio, E.A. Elster, D.M. Burmeister, L.F. Rose, S. Natesan, R. K. Chan, R.J. Christy, K.K. Chung, Burn wound healing and treatment: review and advancements, Crit. Care 19 (2015) 1–12.
[3] B. Allengranzi, S. Nejad, C. Combescure, W. Graafmans, H. Attar, L. Donaldson, D. Pittet, Burden of endemic healthcare associated infection in developing countries: systematic review and metal analysis, Lancet 377 (9761) (2001) 228–241.
[4] T. Bjarnsholt, K. Kirketerp-Møller, P.Ø. Jensen, K.G. Madsen, R. Phipps, K. Krogfelt, N. Høiby, M. Givskov, Why chronic wounds will not heal: a novel hypothesis, Wound Repair Regen. 16 (1) (2008) 2–10.
[5] M. Wojcik, P. Kazimierczak, V. Vivcharenko, M. Koziol, A. Przekora, Effect of vitamin C/hydrocortisone immobilization within curdlan-based wound dressings on In vitro cellular response in context of the management of chronic and burn wounds, Int. J. Mol. Sci. 22 (21) (2021) 11474.
[6] M. Maaz Arif, S.M. Khan, N. Gull, T.A. Tabish, S. Zia, R. Ullah Khan, S.M. Awais, M. Arif Butt, Polymer-based biomaterials for chronic wound management: promises and challenges, Int. J. Pharm. 598 (2021) 120270.
[7] S. Homaeigohar, A.R. Boccaccini, Antibacterial biohybrid nanofibers for wound dressings, Acta Biomater. 107 (2020) 25–49.
[8] Y. Zhu, Y. Matsumura, M. Velayutham, L.M. Foley, T.K. Hitchens, W.R. Wagner, Reactive oxygen species scavenging with a biodegradable, thermally responsive hydrogel compatible with soft tissue injection, Biomaterials 177 (2018) 98–112.
[9] R. Zhao, H. Liang, E. Clarke, C. Jackson, M. Xue, Inflammation in chronic wounds, Int. J. Mol. Sci. 17 (12) (2016) 2085.
[10] C.K. Stover, X.Q. Pham, A.L. Erwin, S.D. Mizoguchi, P. Warrener, M.J. Hickey, F.S. L. Brinkman, W.O. Hufnagle, D.J. Kowalik, M. Lagrou, R.L. Garber, L. Goltry, E. Tolentino, S. Westbrock-Wadman, Y. Yuan, L.L. Brody, S.N. Coulter, K.R. Folger, A. Kas, K. Larbig, R. Lim, K. Smith, D. Spencer, G.- K.-S. Wong, Z. Wu, I.T. Paulsen, J. Reizer, M.H. Saier, R.E.W. Hancock, S. Lory, M.V. Olson, Complete genome sequence of Pseudomonas aeruginosa PAO1, an opportunistic pathogen, Nature 406 (6799) (2000) 959–964.
[11] M.T.T. Thi, D. Wibowo, B.H. Rehm, Pseudomonas aeruginosa biofilms, Int. J. Mol. Sci. 21 (22) (2020) 8671.
[12] Y. Zou, C. Liu, H. Zhang, Y. Wu, Y. Lin, J. Cheng, K. Lu, L. Li, Y. Zhang, H. Chen, Three lines of defense: a multifunctional coating with anti-Adhesion, Bacteria-Killing and anti-Quorum sensing properties for preventing biofilm formation of Pseudomonas aeruginosa, Acta Biomater. 151 (2022) 254–263.
[13] S.R. Shrivastava, P.S. Shrivastava, J. Ramasamy, World health organization releases global priority list of antibiotic-resistant bacteria to guide research, discovery, and development of new antibiotics, J. Med. Soc. 32 (1) (2018) 76.
[14] S. Alven, B.A. Aderibigbe, Chitosan and cellulose-based hydrogels for wound management, Int. J. Mol. Sci. 21 (24) (2020) 9656.
[15] N. Bodenberger, D. Kubiczek, D. Halbgebauer, V. Rimola, S. Wiese, D. Mayer, A. A. Rodriguez Alfonso, L. Ständker, S. Stenger, F. Rosenau, Lectin-functionalized composite hydrogels for "Capture-and-Killing" of carbapenem-resistant Pseudomonas aeruginosa, Biomacromolecules 19 (7) (2018) 2472–2482.
[16] D. Kubiczek, C. Flaig, H. Raber, S. Dietz, A.-K. Kissmann, T. Heerde, N. Bodenberger, A. Wittgens, M. González-Garcia, F. Kang, O.L. Franco, L. Staendker, A.J. Otero-González, P. Walther, K.E. Gottschalk, T. Weil, F. Rosenau, A cerberus-inspired anti-infective multicomponent gatekeeper hydrogel against infections with the emerging "Superbug" yeast Candida auris, Macromol. Biosci. 20 (4) (2020).
[17] H. Yang, Y. Liang, J. Wang, Q. Li, Q. Li, A. Tang, Y. Liu, H.-B. Liu, Multifunctional wound dressing for rapid hemostasis, bacterial infection monitoring and photodynamic antibacterial therapy, Acta Biomater. 135 (2021) 179–190.
[18] M. Wojcik, P. Kazimierczak, A. Benko, K. Palka, V. Vivcharenko, A. Przekora, Superabsorbent curdlan-based foam dressings with typical hydrocolloids properties for highly exuding wound management, Mater. Sci. Eng. C 124 (2021) 112068.
[19] B. Akin, M.M. Ozmen, Antimicrobial cryogel dressings towards effective wound healing, Prog. Biomater. 11 (4) (2022) 331–346.
[20] G. Chen, Y. Yu, X. Wu, G. Wang, J. Ren, Y. Zhao, Bioinspired multifunctional hybrid hydrogel promotes wound healing, Adv. Funct. Mater. 28 (33) (2018) 1801386.
[21] S. Cheng, Y. Jin, N. Wang, F. Cao, W. Zhang, W. Bai, W. Zheng, X. Jiang, Self-adjusting, polymeric multilayered roll that can keep the shapes of the blood vessel scaffolds during biodegradation, Adv. Mater. 29 (28) (2017) 1700171.
[22] X. Yang, J. Yang, L. Wang, B. Ran, Y. Jia, L. Zhang, G. Yang, H. Shao, X. Jiang, Pharmaceutical intermediate-modified gold nanoparticles: against multidrug-resistant bacteria and wound-healing application via an electrospun scaffold, ACS Nano 11 (6) (2017) 5737–5745.
[23] S. Yao, Y. Zhao, Y. Xu, B. Jin, M. Wang, C. Yu, Z. Guo, S. Jiang, R. Tang, X. Fang, S. Fan, Injectable Dual-Dynamic-Bond Cross-Linked Hydrogel for Highly Efficient Infected Diabetic Wound Healing, Adv. Healthc. Mater. 11 (14) (2022) 2200516.
[24] Q. Mao, O. Hoffmann, K. Yu, F. Lu, G. Lan, F. Dai, S. Shang, R. Xie, Self-contracting oxidized starch/gelatin hydrogel for noninvasive wound closure and wound healing, Mater. Des. 194 (2020) 108916.
[25] R.S. Ambekar, B. Kandasubramanian, Advancements in nanofibers for wound dressing: a review, Eur. Polym. J. 117 (2019) 304–336.
[26] G.N. Grover, J. Lam, T.H. Nguyen, T. Segura, H.D. Maynard, Biocompatible hydrogels by oxime click chemistry, Biomacromolecules 13 (10) (2012) 3013–3017.
[27] M. Farahani, A. Shafiee, Wound healing: from passive to smart dressings, Adv. Healthc. Mater. 10 (16) (2021) 2100477.
[28] A. Francesko, P. Petkova, T. Tzanov, Hydrogel dressings for advanced wound management, Curr. Med. Chem. 25 (41) (2018) 5782–5797.
[29] W. Luo, B. Hu, H.-L. Zhang, C. Li, Y. Shi, X. Li, L. Jin, Antibacterial, photothermal and stable Ag-titanium-oxo-clusters hydrogel designed for wound healing, Mater. Des. 226 (2023) 111674.
[30] J. Koehler, F.P. Brandl, A.M. Goepferich, Hydrogel wound dressings for bioactive treatment of acute and chronic wounds, Eur. Polym. J. 100 (2018) 1–11.

[31] M. Kraemer, M. Bellion, A.-K. Kissmann, T. Herberger, C.V. Synatschke, A. Bozdogan, J. Andersson, A. Rodriguez, L. Ständker, S. Wiese, S. Stenger, B. Spellerberg, K.-E. Gottschalk, A. Cetinkaya, J. Pietrasik, T. Weil, F. Rosenau, Aptamers as novel binding molecules on an antimicrobial peptide-armored composite hydrogel wound dressing for specific removal and efficient eradication of Pseudomonas aeruginosa, Int. J. Mol. Sci. 24 (5) (2023) 4800.
[32] A.M. Carmona-Ribeiro, L.D. de Melo Carrasco, Cationic antimicrobial polymers and their assemblies, Int. J. Mol. Sci. 14 (5) (2013) 9906–9946.
[33] H. Du, Y. Wang, X. Yao, Q. Luo, W. Zhu, X. Li, Z. Shen, Injectable cationic hydrogels with high antibacterial activity and low toxicity, Polym. Chem. 7 (36) (2016) 5620–5624.
[34] A. Salomé Veiga, J.P. Schneider, Antimicrobial hydrogels for the treatment of infection, Pept. Sci. 100 (6) (2013) 637–644.
[35] S.R. Nussbaum, M.J. Carter, C.E. Fife, J. DaVanzo, R. Haught, M. Nusgart, D. Cartwright, An economic evaluation of the impact, cost, and medicare policy implications of chronic nonhealing wounds, Value Health 21 (1) (2018) 27–32.
[36] R. Pereira, A. Carvalho, D.C. Vaz, M. Gil, A. Mendes, P. Bártolo, Development of novel alginate based hydrogel films for wound healing applications, Int. J. Biol. Macromol. 52 (2013) 221–230.
[37] V. Vivcharenko, A. Przekora, Modifications of wound dressings with bioactive agents to achieve improved pro-healing properties, Appl. Sci. 11 (9) (2021) 4114.
[38] M. Rezvanian, S.-F. Ng, T. Alavi, W. Ahmad, In-vivo evaluation of Alginate-Pectin hydrogel film loaded with Simvastatin for diabetic wound healing in Streptozotocin-induced diabetic rats, Int. J. Biol. Macromol. 171 (2021) 308–319.
[39] R. Yu, H. Zhang, B. Guo, Conductive biomaterials as bioactive wound dressing for wound healing and skin tissue engineering, Nano-micro Lett. 14 (2022) 1–46.
[40] D. Aycan, B. Selmi, E. Kelel, T. Yildirim, N. Alemdar, Conductive polymeric film loaded with ibuprofen as a wound dressing material, Eur. Polym. J. 121 (2019) 109308.
[41] J. Song, Y. Jung, I. Lee, J. Jang, Fabrication of pDMAEMA-coated silica nanoparticles and their enhanced antibacterial activity, J. Colloid Interface Sci. 407 (2013) 205–209.
[42] W. Yuan, J. Wei, H. Lu, L. Fan, J. Du, Water-dispersible and biodegradable polymer micelles with good antibacterial efficacy, Chem. Commun. 48 (54) (2012) 6857–6859.
[43] D. Keskin, G. Zu, A.M. Forson, L. Tromp, J. Sjollema, P. van Rijn, Nanogels: a novel approach in antimicrobial delivery systems and antimicrobial coatings, Bioact. Mater. 6 (10) (2021) 3634–3657.
[44] T. Manouras, E. Koufakis, E. Vasilaki, I. Peraki, M. Vamvakaki, Antimicrobial hybrid coatings combining enhanced biocidal activity under visible-light irradiation with stimuli-renewable properties, ACS Appl. Mater. Interfaces 13 (15) (2021) 17183–17195.
[45] D. Gokkaya, M. Topuzogullari, T. Arasoglu, K. Trabzonlu, M.M. Ozmen, S. Abdurrahmanoğlu, Antibacterial properties of cationic copolymers as a function of pendant alkyl chain length and degree of quaternization, Polym. Int. 70 (6) (2021) 829–836.
[46] S.K. Samal, M. Dash, S. Van Vlierberghe, D.L. Kaplan, E. Chiellini, C. Van Blitterswijk, L. Moroni, P. Dubruel, Cationic polymers and their therapeutic potential, Chem. Soc. Rev. 41 (21) (2012) 7147–7194.
[47] S.J. Shirbin, S.J. Lam, N.-J.-A. Chan, M.M. Ozmen, Q. Fu, N. O'Brien-Simpson, E. C. Reynolds, G.G. Qiao, Polypeptide-based macroporous cryogels with inherent antimicrobial properties: the importance of a macroporous structure, ACS Macro Lett. 5 (5) (2016) 552–557.
[48] K.M. Zurick, M. Bernards, Recent biomedical advances with polyampholyte polymers, J. Appl. Polym. Sci. 131 (6) (2014).
[49] J. Qiao, Z. Liu, S. Cui, T. Nagy, M.P. Xiong, Synthesis and evaluation of an amphiphilic deferoxamine: gallium-conjugated cationic random copolymer against a murine wound healing infection model of Pseudomonas aeruginosa, Acta Biomater. 126 (2021) 384–393.
[50] M. TopuzoĞullari, Effect of polyelectrolyte complex formation on the antibacterial activity of copolymer of alkylated 4-vinylpyridine, Turk. J. Chem. 44 (3) (2020) 634–646.
[51] R. Song, M. Murphy, C. Li, K. Ting, C. Soo, Z. Zheng, Current development of biodegradable polymeric materials for biomedical applications, Drug Des Devel. Ther. (2018) 3117–3145.
[52] L.Q. Xu, N.N. Li, J.C. Chen, G.D. Fu, E.-T. Kang, Quaternized poly (2-(dimethylamino) ethyl methacrylate)-grafted agarose copolymers for multipurpose antibacterial applications, RSC Adv. 5 (76) (2015) 61742–61751.
[53] E. Koufakis, T. Manouras, S.H. Anastasiadis, M. Vamvakaki, Film properties and antimicrobial efficacy of quaternized PDMAEMA brushes: short vs long alkyl chain length, Langmuir 36 (13) (2020) 3482–3493.
[54] J. Huang, H. Murata, R.R. Koepsel, A.J. Russell, K. Matyjaszewski, Antibacterial polypropylene via surface-initiated atom transfer radical polymerization, Biomacromolecules 8 (5) (2007) 1396–1399.
[55] A. Kumar, J. Sharma, P. Srivastava, L. Nebhani, Mechanically robust and highly bactericidal macroporous polymeric gels based on quaternized N, N-(dimethylamino) ethyl methacrylate possessing varying alkyl chain lengths, J. Mater. Chem. B 11 (10) (2023) 2234–2248.
[56] Y. Jiao, L.-N. Niu, S. Ma, J. Li, F.R. Tay, J.-H. Chen, Quaternary ammonium-based biomedical materials: state-of-the-art, toxicological aspects and antimicrobial resistance, Prog. Polym. Sci. 71 (2017) 53–90.
[57] M. Krämer, A.-K. Kissmann, H.F. Raber, H.u. Xing, P. Favella, I. Müller, B. Spellerberg, T. Weil, D. Kubiczek, S. Sihler, U. Ziener, F. Rosenau, Bsa hydrogel beads functionalized with a specific aptamer library for capturing pseudomonas aeruginosa in serum and blood, Int. J. Mol. Sci. 22 (20) (2021) 11118.
[58] C.R. Kruse, M. Singh, S. Targosinski, I. Sinha, J.A. Sørensen, E. Eriksson, K. Nuutila, The effect of pH on cell viability, cell migration, cell proliferation, wound closure, and wound reepithelialization: in vitro and in vivo study, Wound Repair Regen. 25 (2) (2017) 260–269.
[59] A. Gorman, A.P. Golovanov, Lipopolysaccharide structure and the phenomenon of low endotoxin recovery, Eur. J. Pharm. Biopharm. 180 (2022) 289–307.
[60] R. Lambert, G. Hanlon, S.P. Denyer, The synergistic effect of EDTA/antimicrobial combinations on Pseudomonas aeruginosa, J. Appl. Microbiol. 96 (2) (2004) 244–253.